Enhancement of the efficiency in green organic light-emitting devices utilizing multiple heterostructures acting as a hole transport layer

D. C. Choo, D. U. Lee, Y. B. Yoon, T. W. Kim, J. H. Kim[1], J. H. Seo[2], and Y. K. Kim[2]

Research Institute of Information Display, Division of Electronics and Computer Engineering, Hanyang University, Seoul 133-791, Korea

[1]Department of Electronic Engineering, Hong-ik University, Seoul 121-791, Korea

[2]Department of Information Display Engineering & COMID, Hong-ik University, Seoul 121-791, Korea

Phone: +82-2-2220-0354, E-mail: fallchoo@hanyang.ac.kr

Abstract

The electrical and the optical properties of organic light-emitting devices (OLEDs), with and without various kinds of multiple heterostructures were investigated. The efficiency in green OLEDs were significantly enhanced by the structure of the multiple heterostructures acting as a hole transport layer (HTL) rather than by the number of periods. These results indicate that highly efficient green OLEDs utilizing multiple heterostructures acting as a HTL can be fabricated.

I. Introduction

Organic light-emitting devices (OLEDs) have also been very attractive due to their promising applications, which offer many advantages of low driving voltage, low power consumption, high contrast, wide viewing angle, low cost, and fast response [1-6]. Recently, OLEDs with multiple heterostructures have been used to achieve narrower spectral emission, higher emission efficiency, and tunable emission spectra [7, 8]. Even though some works on OLEDs have proposed using multiple heterostructures to enhance their efficiencies [9, 10], systematic studies concerning the Enhancement of the efficiency in green OLEDs utilizing various kinds of multiple heterostructures have not been reported yet because of the complicated device-fabrication process.

This presentation reports the electrical and the optical properties of OLEDs utilizing multiple heterostructures deposited by using organic molecular-beam deposition (OMBD). Current density-voltage, luminance-voltage, efficiency-current density, and electroluminescence (EL) measurements were carried out to investigate the efficiency and the color stabilization of the aluminum (Al)/lithium quinolate (Liq)/tris (8-hydroxyquinoline) aluminum (Alq_3)/multiple heterostructures/N, N′-bis-(1-naphthyl)-N, N′-diphenyl-1,1′-biphenyl-4,4′-diamine (NPB)/indium-tin-oxide (ITO)/glass structures with and without various kinds of multiple heterostructures. The multiple heterostructures consisted of NPB with 5,6,11,12-tetraphenylnaphthacene (rubrene) and of NPB with mixed rubrene:NPB.

II. Experimental Details

The sheet resistivity of the ITO thin films coated on glass substrates used in this study was 15 Ω/□. The ITO substrates were cleaned using acetone and methanol at 60°C for 5 min, and rinsed in de-ionized water thoroughly. After the chemically cleaned ITO substrates had been dried by using N_2 gas with a purity of 99.9999%, the substrates were treated with an oxygen plasma for 10 min. The four kinds of samples used in this study were deposited on ITO thin films coated on glass substrates by using OMBD with effusion cells and shutters and consisted of the following structures from the top: an Al (100 nm) cathode electrode, a Liq (2 nm) electron injection layer (EIL), an Alq_3 (60 nm) electron transport layer,

either no layer, a layer consisting of 3 or 5 periods of NPB/rubrene, or a layer consisting of 3 periods of NPB/mixed rubrene:NPB, a NPB (10 nm) hole transport layer, an ITO anode electrode, and the glass substrate. The fabricated Al/Liq/Alq_3/multiple heterostructures/NPB/ITO/glass structures without the multiple heterostructures, with 3 periods of NPB/rubrene, with 3 periods of NPB/mixed rubrene:NPB, and with 5 periods of NPB/rubrene are denoted as devices I, II, III, and IV, respectively. The total thickness of the NPB/rubrene or NPB/mixed rubrene:NPB multiple heterostructures was approximately 40 nm. The NPB/rubrene multiple heterostructure layer was used to lower the mobility of holes due to the existence of the rubrene molecules, which act as hole traps in the OLEDs [11]. The Liq layer is used as an EIL, leading to a lower turn-on voltage and a higher power efficiency [12]. The depositions of the OLED layers were done at a substrate temperature of 27°C and a system pressure of 5×10^{-6} Torr. The growth rates of the organic layers and the metal layers were approximately 0.1 and 0.5 Å/s, respectively. The mixing process for the rubrene:NPB layers was carried out by using co-evaporation with a 1:1 growth rate of the rubrene and the NPB molecules. The emitting area was 5×5 mm^2. Standard OLEDs, Al/Liq/Alq_3/NPB/ITO devices, without multiple heterostructures were grown for comparison with the OLEDs with NPB/rubrene or NPB/mixed rubrene:NPB multiple heterostructures. The structures of the OLEDs fabricated in this work are summarized in Table. I.

III. Results and Discussion

Figure 1 shows the schematic energy band diagrams of the fabricated OLEDs of devices (a) II, III, and (c) IV. The highest occupied molecular orbital (HOMO) and the lowest unoccupied molecular orbital (LUMO) levels of the rubrene are -5.4 and -3.2 eV, respectively [13], and the HOMO and the LUMO levels of the NPB layer, as obtained by using cyclic voltammetry, are -5.5 and -2.5 eV, respectively [13]. Both the HOMO and the LUMO states of the rubrene wells are found to be surrounded by the NPB barriers. Since the holes are trapped and accumulated in the HOMO levels of the NPB/rubrene quantum wells of the OLEDs due to the existence of barriers at the NPB/rubrene heterointerfaces, the mobility of the holes in the multiple heterostructures acting as a HTL decreases, resulting in an enhanced efficiency of the OLEDs due to a better balance between the number of electrons and the number of holes. The recombination probability in the NPB/rubrene multiple heterostructures and at the NPB/Alq_3 heterointerface increases due to the improved balance between the electrons and the holes. The electrical and the optical properties of the OLEDs are significantly affected by their periods and compositions.

Figure 2 shows (a) the current densities as functions of the applied voltage, (b) the luminances as functions of the applied voltage, and (c) the efficiencies as functions of the current density for the OLEDs with various structures. The inset in Figure 2(a) shows the reverse leakage current at the reverse bias conditions. Filled rectangles, circles, upright triangles, and inverted triangles represent the OLEDs of devices I, II, III, and IV, respectively. The current density-voltage characteristics in the reverse bias regions of the OLEDs with multiple heterostructures acting as a HTL show almost similar behaviors. Therefore, the injection and the transport of the holes are significantly affected by the structures of the HTL. The luminance and the efficiency of device III are the highest among the devices. The enhancement of the luminance and the efficiency for device III originates from a better balance between the holes and the electrons at the NPB/Alq_3 heterointerface acting as an emitting region due to the existence of the mixed multiple heterostructures rather than from an increase in the periods of the multiple heterostructures. The maximum efficiency and the luminance of device III at 80 mA/cm^2 are 3.5 cd/A and 2800 cd/m^2, respectively. While the high efficiencies of devices III and VI are stable regardless of the variation in the current density, which is similar to that of device I, the low efficiency of device II is also stable. Because the holes moving within the multiple heterostructures for device II are significantly accumulated at the NPB/rubrene heterointerfaces due to the thickness of the NPB layer, being larger than it is in device IV, the

holes emitted from the ITO anode for device II are captured in large numbers in the NPB/rubrene heterointerfaces during the transport of the holes in the heterostructures. Since the turn-on voltages of devices I, II, III, and IV are 2.6, 2.7, 2.5 and 2.6 V, respectively, the turn-on voltages of four fabricated OLEDs are almost the same, regardless of the structure of the HTL.

IV. Summary and Conclusions

The electrical and the optical properties of the OLEDs were significantly affected by the existence of various kinds of multiple heterostructures acting as a HTL. The OLEDs of device III showed the highest efficiencies. The turn-on voltages of fabricated OLEDs were almost the same, regardless of the structure of the HTL. The efficiency in green OLEDs was significantly enhanced by the structure of the multiple heterostructures acting as a HTL rather than by the number of periods. These present results can help improve understanding of the fabrication of highly efficient and color-stabilized green OLEDs utilizing NPB/mixed rubrene:NPB multiple heterostructures acting as a HTL.

Acknowledgement

This work was supported by the Korea Research Foundation Grant funded by the Korean Government (MOEHRD) (KRF-2004-015-D00166).

References

[1] C. W. Tang and S. A. Van Slyke, Appl. Phys. Lett. **51**, 913 (1987).
[2] P. E. Burrows, S. R. Forrest, S. P. Sibley, and M. E. Thompson, Appl. Phys. Lett. **69**, 2959 (1996).
[3] R. H. Friend, R. W. Gymer, A. B. Holmes, J. H. Burroughes, R. N. Marks, C. Taliani, D. D. C. Bradley, D. A. Dos Santos, J. L. Bredas, M. Löglund, and W. R. Salaneck, Nature **397**, 121 (1999).
[4] H. Aziz, Z. D. Popovic, N-X. Hu, A-M. Hor, and G. Xu, Science **283**, 1900 (1999).
[5] M. A. Baldo, M. E. Thompson, and S. R. Forrest, Nature **403**, 750 (2000).
[6] M. A. Baldo and S. R. Forrest, Phys. Rev. B **62**, 10958 (2000).
[7] J. Huang, K. Yang, Z. Xie, B. Chen, H. Jiang, and S. Liu, Appl. Phys. Lett. **73**, 3348 (1998).
[8] Y. Qiu, Y. Gao, L. Wang, P. Wei, L. Duan, D. Zhang, and G. Dong, Appl. Phys. Lett. **81**, 3540 (2002).
[9] G. He, O. Schneider, D. Qin, X. Zhou, M. Pfeiffer, and K. Leo, J. Appl. Phys. **90**, 5773 (2004).
[10] Y. Yuan, D. Grozea, and Z. H. Lu, Appl. Phys. Lett. **86**, 143509 (2005).
[11] H. Aziz and Z. D. Popovic, Appl. Phys. Lett. **80**, 2180 (2002).
[12] Z. Liu, O. V. Salata, and N. Male, Synth. Met. **128**, 211 (2002).
[13] Y. Hamada. H. Kanno, T. Tsujioka, H. Takahashi, and T. Usuki, Appl. Phys. Lett. **75**, 1682 (1999).

Table I. Structures of the OLEDs fabricated in this study.

Device / Layer	I	II	III	IV
Cathode	Al (100 nm)			
EIL	Liq (2 nm)	Liq (2 nm)	Liq (2 nm)	Liq (2 nm)
ETL/EML	Alq_3 (60 nm)			
Heterostructures	NPB (50 nm)	[NPB (10.3 nm) / Rubrene (3 nm)]$_3$	[NPB (10.3 nm) / mixed Rubrene:NPB (3nm)]$_3$	[NPB (5 nm) / Rubrene (3 nm)]$_5$
HTL		NPB (10 nm)	NPB (10 nm)	NPB (10 nm)
Anode	ITO			
Substrate	Glass			

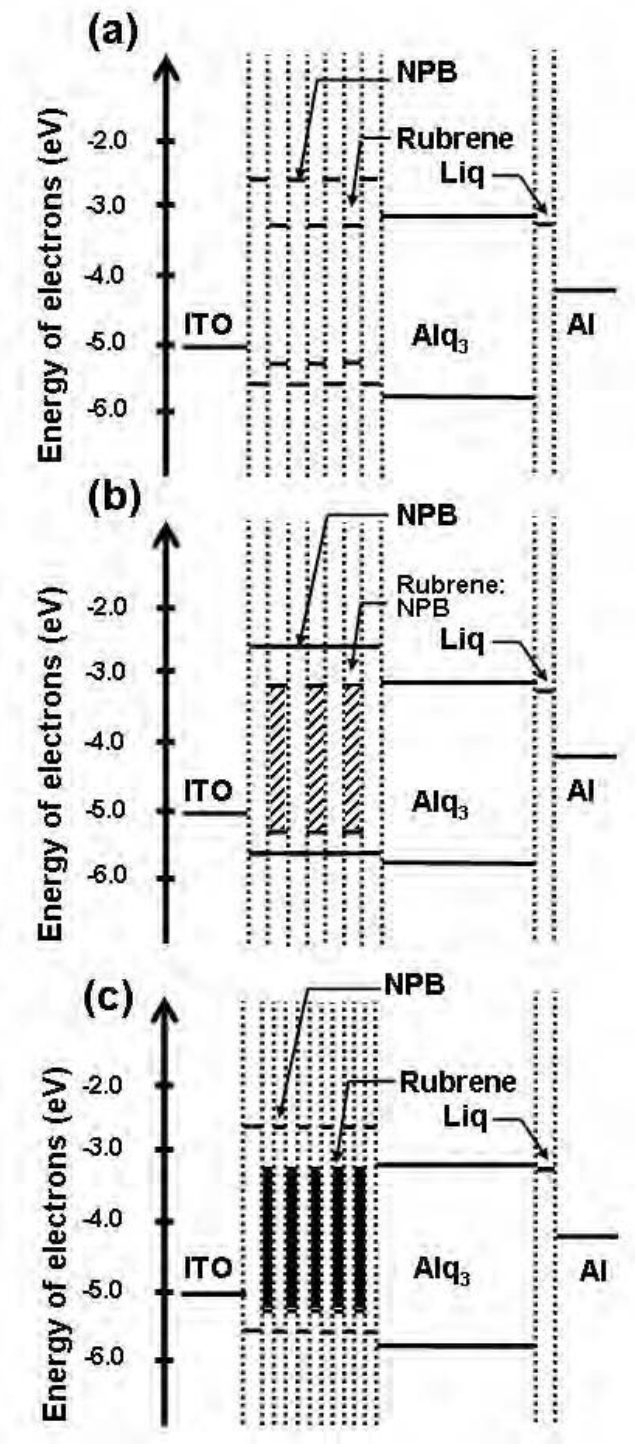

Figure 1. Schematic energy band diagrams of the OLEDs of devices (a) II, (b) III, and (c) IV.

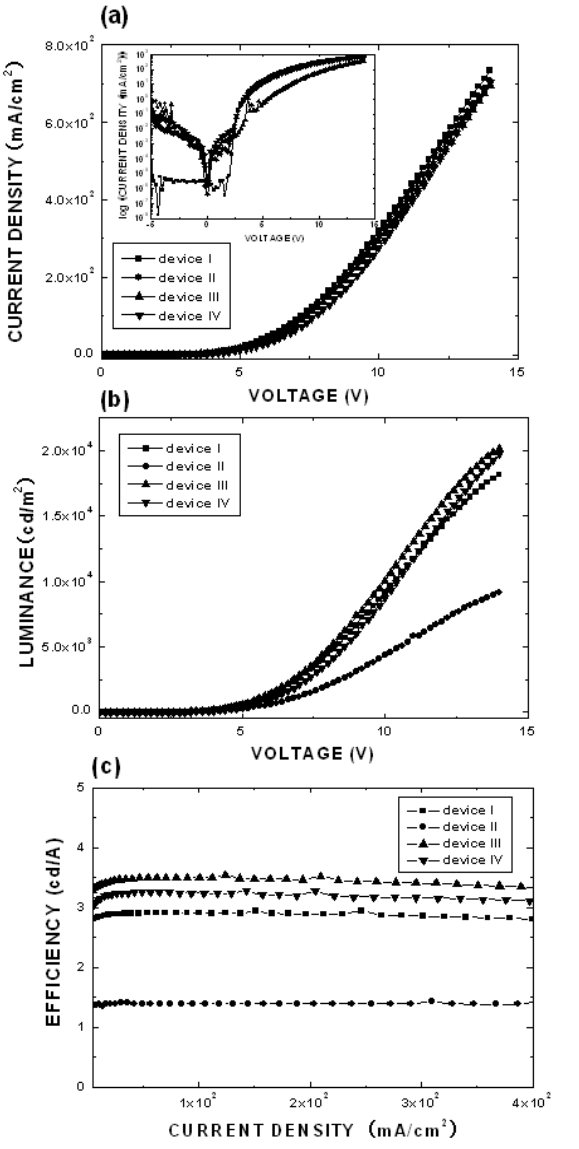

Figure 2. (a) Current densities as functions of the applied voltage, (b) luminances as functions of the applied voltage, and (c) efficiencies as functions of the current density for OLEDs with various kinds of multiple heterostructures. The insert of Fig. 1(a) indicates the log current densities as functions of the applied voltage from -5 V to 14 V. Filled rectangles, circles, upright triangles, and inverted triangles represent the OLEDs of devices I, II, III, and IV, respectively.